30 From mushrooms to isolas: surprising behaviour in a simple biosynthetic system subject to end-product inhibition

J.-H.S. Hofmeyr, B.G. Olivier and J.M. Rohwer
Dept. of Biochemistry, University of Stellenbosch, Private Bag X1, Matieland 7602, South Africa

Introduction

Since the discovery of metabolic feedback in the form of end-product inhibition of an allosteric enzyme upstream from the end-product [1,2] an extensive body of literature has been built up around the mathematical and computer modelling of this phenomenon. To our knowledge the allosteric enzymes in these model feedback systems have usually been represented by rate equations derived from irreversible reaction mechanisms such as the Monod-Wyman-Changeux (MWC) equation [3], the Adair equation [4] or the Hill equation [5] (due its complexity the Koshland-Nemethy-Filmer equation [6] has been little used, if at all). Other rate equations have been developed to explain cooperativity but usually do not incorporate allosteric end-product inhibition [7]. The generalisation that most allosteric enzymes catalyse reactions with large equilibrium constants seemed to serve as a justification for ignoring possible inhibition effects by the direct reaction product, whether thermodynamic (mass action) or kinetic (competition with substrate for binding to the active site). However, it is not the equilibrium constant *per se* but the disequilibrium ratio (mass-action ratio/equilibrium constant) that determines to which degree the product will affect reaction rate by mass-action (for an example of the dangers of ignoring this, see the paper by Cornish-Bowden and Cárdenas in this volume, p. 65); the current paper serves as another such reminder).

Only in the late 1970s, in a four-part study [9–12], did Popova and Sel'kov extend the MWC equation to cover reversible reaction mechanisms. However, to the best of our knowledge, this important work has largely been ignored and certainly not used in modelling. Because the Hill-equation has definite advantages for modelling (such as (i) fewer parameters, and (ii) parameters that have a clear operational meaning) we developed a reversible Hill equation that incorporates

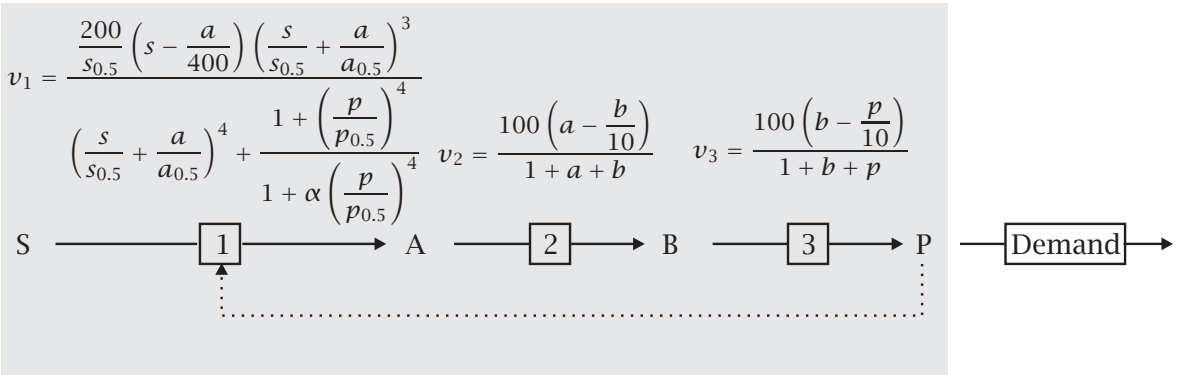

Fig. 30.1 *A supply-demand system in which the first enzyme of the 3-step supply is subject to end-product inhibition.* The supply system is contained in the shaded area and it is its steady-state flux response to variation in the concentration of P that is simulated. The rate of E_1 is described by the reversible Hill equation with one allosteric modifier [8]. In all simulations of this system the $s_{0.5}$-value of E_1 was 1 mM; the concentration of S was also clamped at 1 mM. The strength of inhibition factor α was set to 0.01. The rate equations for the other supply enzymes are instances of the reversible Michaelis-Menten equation $v = \frac{V_f}{K_s}\left(s - \frac{p}{K_{eq}}\right) \Big/ \left(1 + \frac{s}{K_s} + \frac{p}{K_p}\right)$. For all reactions K_s and K_p were set to 1 mM and therefore have been omitted from the rate equations.

allosteric modulator effects, starting from a reversible Adair binding mechanism [8]. This equation shares an interesting feature with the reversible MWC equation [9] (and with the parent Adair equation): besides the usual mass-action and competitive inhibitory effects, the product can also activate the enzyme. Microscopic reversibility in the mechanism requires that binding of product enhances not only subsequent product binding, but also subsequent substrate binding, making this activation effect unavoidable. Mathematically all three product effects are clearly visible in the rate equation (see, for example, the functional positions of product concentration a in the rate equation for step 1 in Fig. 30.1): The inhibitory mass-action effect is due to the numerator term $(s - \frac{a}{400})$, competitive inhibition by A is possible because its concentration occurs as a positive term in the denominator, while activation by A is possible because its concentration occurs as a positive term in the numerator.

In this paper we ask the questions: How do these direct product effects affect the system in practice? How is the behaviour of the supply system affected? An attempt to answer these questions allows us to evaluate not only the relative contribution of the various product effects on the behaviour of the system, but also the role of the downstream enzymes in setting the steady-state value of the product concentration. In this paper we shall treat only steady-state behaviour and not time-dependent phenomena.

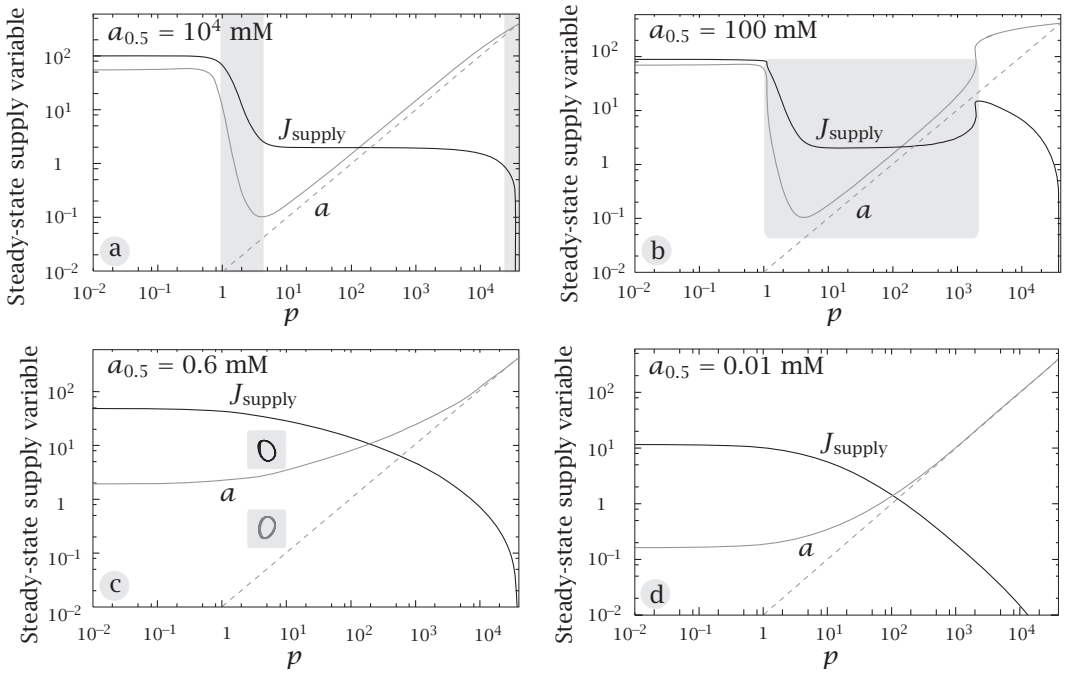

Fig. 30.2 *Response of the supply flux and steady-state concentration of A to changing p at different values of $a_{0.5}$, the half-saturation constant of* E_1 *for its immediate product A.* Simulation conditions were as in Fig. 30.1; the values of $a_{0.5}$ are shown on the graphs. Flux units are mM.min^{-1} and concentration units are mM. The dotted line is the theoretical equilibrium value of a as it varies with p ($p_{\text{eq}}/a_{\text{eq}} = K_2K_3 = 100$). In graph *a* the shaded bands show two regions where the supply flux responds sensitively to P: the leftmost one a far-from-equilibrium region and the rightmost one a near-equilibrium region (for this system the equilibrium concentration of P at $s = 1$ mM is 4×10^4 mM.). In graph *b* the shaded block delineates a region flanked by hysteretic responses, forming a so-called *mushroom*. In graph *c* the mushroom has pinched off to form the shaded closed-form response called an *isola*. In graph *d* the isola has vanished, leaving a typical competitive product-inhibition flux-response curve. Simulations were performed with Scamp [13] using its continuation algorithm.

Simulation study

Fig. 30.1 is a scheme of the system studied (the so-called 'Stellenbosch organism'). We considered only the steady-state response of the shaded supply block to changes in the 'end-product' P. This allowed us to construct supply characteristics, which could then be used in a supply-demand analysis of the full system (such as described in [14]). We performed a digital experiment in which the steady-state of the supply was calculated for a series of P concentrations, from zero to its equilibrium value of 4×10^4 mM, at a fixed S concentration of 1 mM. To study the effect of the accompanying variation in the steady-state concentration of A on its producing enzyme E_1, the experiment was repeated for different half-effect concentrations $a_{0.5}$, from 10^4 mM (weak binding of A to E_1) to 0.01 mM (strong

binding of A to E_1). The results are shown in Fig. 30.2.

In Fig. 30.2A E_1 is kinetically-speaking practically insensitive to A. Most of the supply flux characteristic is completely determined by the inhibitory effect of P; only at very high, near-equilibrium concentrations of P does a become high enough to inhibit step 1 through mass action (the contribution of the mass-action term in the elasticity coefficient $\varepsilon_a^{v_1}$ will be more negative than -1 only at a-values greater than 200 mM under these simulation conditions). For most of the range of p-variation the E_2-E_3 reaction block is near equilibrium (as shown by the close proximity of the steady-state concentration of A and its calculated equilibrium value with respect to P, shown by the dashed line). Starting at equilibrium p, a decreases with p. However, at the point where the flux starts increasing because end-product inhibition by P weakens (shown by the left-hand shaded band), a increases sharply. The reason for this is that the degree of saturation of E_2 by A must increase to sustain the concomitant flux-increase that occurs in that region of p. The prediction that the higher the V_{max} of E_2, the less the increase in a needed to match the flux-increase, and therefore the lower the plateau in a, has been confirmed by simulation (results not shown). From a regulatory point of view [14] the flux behaviour in Fig. 30.2A is ideal in that it shows a sensitive response in a narrow, far-from-equilibrium range of p around $p_{0.5}$, with the flux-response profile solely due to cooperative end-product inhibition.

When the strength of binding of A to E_1 increases a point is reached where the activation effect of A on E_1 becomes visible (the right-hand side of the shaded area in Fig. 30.2B). Here both J_{supply} and a respond hysterically to p. Close inspection reveals that the curves also become hysteretic at the left-hand side of the shaded area (this is more visible in Fig. 30.3). Such a double hysteresis is known as a *mushroom* [15], albeit it an upside-down mushroom in this instance.

A further increase in the strength of binding of A to E_1 magnifies the mushroom profile until a point is reached where the mushroom pinches off to form an *isola* [15] (see Fig. 30.3, which illustrates this effect clearly). The remaining stable monotonic rate curve is determined solely by competitive inhibition of E_1 by A and, at high p, also by mass-action. Although the isola has stable sections (so that, in principle at least, the system could exist in a steady state on the isola) enough variation in p will invariably cause a jump onto the monotonic steady-state curve.

Finally, when A binds very strongly to E_1, the isola vanishes and the observed flux response is determined solely by the competitive inhibitory effect of A, which effectively swamps both end-product inhibition by P and the activatory effect of A. Here the flux response of the supply to p has lost its regulatory properties.

Discussion

This study arose from an attempt to design a regulated metabolic system bottom-up from first principles [14,16]. The rather exotic kinetic behaviour described

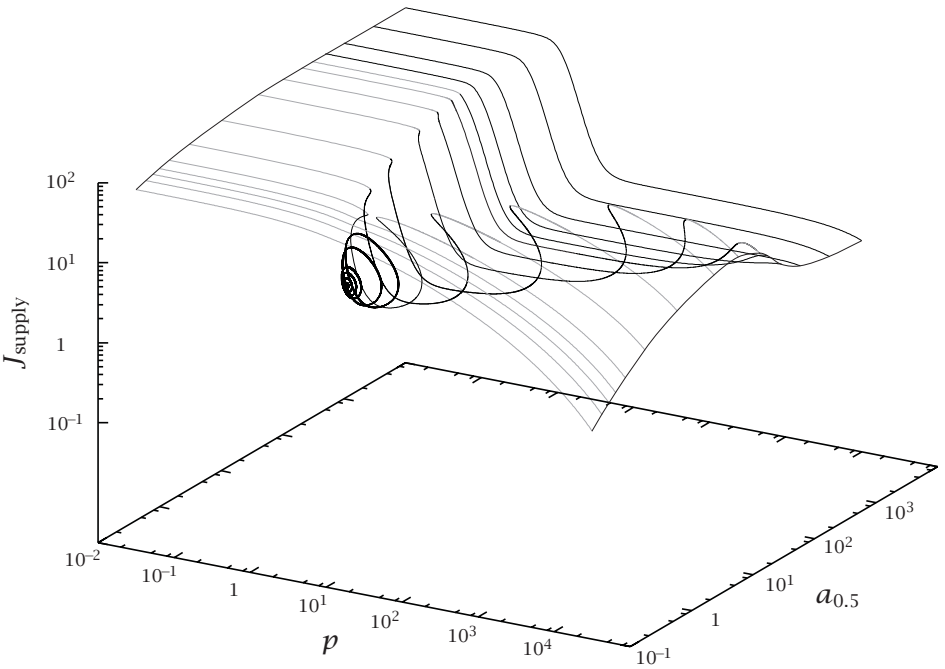

Fig. 30.3 *A 3-dimensional representation of the mushroom transforming into a vanishing isola, with supply flux plotted against p at different values of* $a_{0.5}$. Similar graphs can be constructed for the steady-state concentrations a or b: the shapes of the mushrooms and the isolas are different, but on the whole the same picture is obtained.

above was discovered rather than predicted. Note that this type of simple negative feedback system has been the subject of numerous studies; the study described here differed only in that a more general reversible rate equation was used for the allosteric enzyme. This introduced the possibility of rate activation by immediate product. Product activation is not a common phenomenon and only a few examples are known, such as the inhibition of NADH-dependent nitrite reductase from *Escherichia coli* by NAD [17], but these examples do not seem to be explainable in terms of the mechanisms of the sort considered here. Because it is a possible source of instability one would expect most occurrences of it during evolution to have been eliminated by selection. Despite this, the study still serves as a lesson in the dangers of making limiting assumptions about the behaviour of a model system.

The hysteretic behaviour also leads to a number of other important issues, such as oscillatory behaviour, the possibility of metabolic switches, and issues of stability. These aspects are under investigation and will be published elsewhere.

Although space constraints prevent us from exploring this matter in detail, the role of the intermediate enzymes E_2 and E_3 in determining the steady-state concentration of A and, therefore, the effect of A on E_1 should also be considered in analysing the overall behaviour of this system (see [14,16]). In fact, in any experimental search for this type of behaviour, using, for example, reconstituted

enzyme systems, variation in the activities of E_2 and E_3 can be used to vary a (the variation of $a_{0.5}$—possible in experiments *in silico*—not being feasible experimentally).

This paper again illustrates how useful modelling can be to discover new forms of metabolic behaviour, although the phenomena described here have not yet been looked for in real systems. An example of where modelling led to the discovery of a new type of behaviour which was subsequently found to exist in the real system is given by Poolman and Fell (this volume, p. 249), who describe the existence of two steady states in the Calvin cycle.

References

1. Novick, A. and Szilard, L. (1954) In *Dynamics of Growth Processes* (Bonner, D., ed.), Princeton University Press.
2. Yates, R. A. and Pardee, A. B. (1956). *J. Biol. Chem.* **221**, 757–770.
3. Monod, J., Wyman, J., and Changeux, J.-P. (1965) *J. Mol. Biol.* **12**, 88–118.
4. Adair, G. (1925) *J. Biol. Chem.* **63**, 529–545.
5. Hill, A. (1910) *J. Physiol. (London)* **40**, iv–vii.
6. Koshland, Jr., D. E., Nemethy, G., , and Filmer, D. (1966) *Biochemistry* **5**, 365–385.
7. Cornish-Bowden, A. (1995) *Fundamentals of enzyme kinetics*. Portland Press, London, 2nd edition.
8. Hofmeyr, J.-H. S. and Cornish-Bowden, A. (1997) *Comp. Appl. Biosci.* **13**, 377–385.
9. Popova, S. V. and Sel'kov, E. E. (1975) *FEBS Lett.* **53**, 269–273.
10. Popova, S. V. and Sel'kov, E. E. (1976) *Mol. Biol. (Moskva)* **10**, 1116–1126.
11. Popova, S. V. and Sel'kov, E. E. (1978) *Mol. Biol. (Moskva)* **13**, 129–139.
12. Popova, S. V. and Sel'kov, E. E. (1978) *Mol. Biol. (Moskva)* **12**, 1139–1151.
13. Sauro, H. M. (1993) *Comp. Appl. Biosci.* **9**, 441–450.
14. Hofmeyr, J.-H. S., Olivier, B. G., and Rohwer, J. M. (2000) Putting the Cart Before the Horse: Designing a Metabolic System in Order to Understand It. In *Technological and Medical Implications of Metabolic Control Analysis*, (Cornish-Bowden, A. and Cárdenas, M. L., eds.), pp. 299–308. Kluwer Academic Publishers, Dordrecht.

15. Murray, J. D. (1989) *Mathematical Biology*. Springer-Verlag, Berlin.

16. Olivier, B. (1999) Designing a 4-Way Metabolic Junction. Master's thesis, University of Stellenbosch.

17. Coleman, K. J., , Cornish-Bowden, A., and Cole, J. A. (1978) *Biochem. J.* **175**, 495–499.